Synthesis, characterization and study of the chromogenic properties of the hybrid polyoxometalates $[PW_{11}O_{39}(SiR)_2O]^{3-}$ (R = Et, $(CH_2)_nCH=CH_2$ (n = 0, 1, 4), $CH_2CH_2SiEt_3$, $CH_2CH_2SiMe_2Ph$) ☆

Dominique Agustin [1], Jérôme Dallery, Cristina Coelho, Anna Proust, René Thouvenot [*]

Laboratoire de Chimie Inorganique et Matériaux Moléculaires, UMR CNRS 7071, Institut de Chimie Moléculaire, FR 2769, Université Pierre et Marie Curie, Paris 6, Case Courrier 42, 4 Place Jussieu, 75252 Paris Cedex 05, France

Abstract

Reaction of Cl_3SiR or $(EtO)_3SiR$ with $[PW_{11}O_{39}]^{7-}$ affords the disubstituted hybrid anions $[PW_{11}O_{39}(SiR)_2O]^{3-}$. These species have been characterized by IR spectroscopy in the solid state and by multinuclear NMR (^1H, ^{29}Si, ^{31}P and ^{183}W) and cyclic voltammetry in solution. The hydrosilylation of $[PW_{11}O_{39}(Si–CH=CH_2)_2O]^{3-}$ has been achieved with Et_3SiH and $PhSiMe_2H$. These are the first examples of hydrosilylation on a hybrid tungstophosphate core. The chromogenic behaviour of hybrid species has been demonstrated in solution.
© 2006 Elsevier B.V. All rights reserved.

Keywords: Polyoxometalates; Multinuclear NMR; Hydrosilylation; Hybrid; Chromogenic properties

1. Introduction

Modification of the colour of matrices by any excitation source (light, electric potential...) remains an important challenge [2–4]. For this purpose, polyoxometalates (POMs) are elected to be valuable objects of investigation. POMs are formed by transition metals in high oxidation state (W^{VI}, Mo^{VI}) surrounded by oxo-ligands [5]. These compounds indeed present interesting electrochemical and photochemical properties [5–7]. The ability of POMs to be reduced is well-known and the "heteropolyblue" anions have been extensively studied [8–12]. POMs can be entrapped into a polymeric network without covalent linkage [13,14] or hybrid POMs can be linked by covalent bonds

to a polymeric network through several copolymerization processes [15]. Numerous works deal with organosilyl derivatives of the tungstosilicates $[SiW_{11}O_{39}]^{8-}$ [14,16] or γ-$[SiW_{10}O_{36}]^{8-}$ [15] while, to our knowledge, $[PW_{11}O_{39}]^{7-}$, hereafter $\{PW_{11}\}$, was surprisingly scarcely used in this field [17]. In order to work on $\{PW_{11}\}$-containing networks, we have achieved the linkage of hybrid tungstophosphates and organosilanes linkers. Some organometallic reactions could be envisaged for extra Si–C couplings. The hydrosilylation process, first investigated by Judeinstein on $[SiW_{11}O_{39}(SiR)_2O]^{4-}$ cores [14], was thought to be efficient to obtain new types of $\{PW_{11}\}$-containing molecular materials relying on covalent bonding.

In this work, we describe the synthesis and thorough characterization of new POM-based compounds, using $[PW_{11}O_{39}(Si–CH=CH_2)_2O]^{3-}$ as precursor and $HSiEt_3$ or $HSiMe_2Ph$ as second-generation grafting agents, linked through hydrosilylation. Electrochemical and chromogenic behaviours of some of these species have also been studied in organic solvent and are presented therein.

2. Results and discussion

2.1. Syntheses of $[Bu_4N]_3[PW_{11}O_{39}(SiR)_2O]$

2.1.1. Hybrid precursors $[Bu_4N]_3[PW_{11}O_{39}(SiR)_2O]$ $(R = Et, (CH_2)_nCH{=}CH_2 \ (n = 0, 1, 4))$

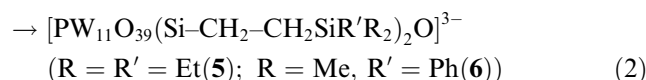The silylated hybrid compounds $[PW_{11}O_{39}(SiR)_2O]^{3-}$ {R = Et (**1**), $(CH_2)_nCH{=}CH_2$ ($n = 0$ (**2**), 1 (**3**), 4 (**4**))} were obtained as tetrabutylammonium salts following two different synthetic procedures. The method (a) (Eq. (1a)) started with the isolation of the mixed salt $(Bu_4N)_4$-$K[H_2PW_{11}O_{39}]$ as a powder by direct addition of tetrabutylammonium bromide to an aqueous solution of $K_7[PW_{11}O_{39}]$ [18,19]. The product was dissolved in acetonitrile and trichloroorganosilane $RSiCl_3$ (R = CH=CH$_2$, CH$_2$–CH=CH$_2$, (CH$_2$)$_4$–CH=CH$_2$) was added. The method (b) consisted in the direct reaction in acetonitrile of a mixture of tetrabutylammonium bromide, $K_7[PW_{11}$-$O_{39}]$, a slight excess of $(EtO)_3SiR$ (R = Et, CH=CH$_2$, CH$_2$–CH=CH$_2$) and four equivalents of aqueous hydrochloric acid under an nitrogen for one night at room temperature (Eq. (1b)). In the method (b), the reaction was a solid/liquid phase-transfer reaction (Fig. 1). These syntheses should be achieved in organic solvent and not in water as it had been previously described for {SiW$_{11}$} analogues [14] in order to slow down the hydrolysis of silanes and minimize resulting polymerization. Except for triethoxyethylsilane, the organosilanes were chosen to possess a terminal reactive vinylic function

$$(Bu_4N)_4KH_2[PW_{11}O_{39}] + 2RSiCl_3 + H_2O$$
$$\rightarrow (Bu_4N)_3[PW_{11}O_{39}(SiR)_2O] + Bu_4NCl + 4HCl + KCl \quad (1a)$$

(R = CH=CH$_2$(**2**), CH$_2$–CH=CH$_2$(**3**), (CH$_2$)$_4$–CH=CH$_2$(**4**))

Fig. 1. Schematic procedure of silanes grafting on $[PW_{11}O_{39}]^{7-}$.

$$K_7[PW_{11}O_{39}] + 2RSi(OR')_3 + 4HCl + H_2O + 3Bu_4NBr$$
$$\rightarrow (Bu_4N)_3[PW_{11}O_{39}(SiR)_2O] + 6R'OH + 4KCl + 3KBr \quad (1b)$$

(R = Et(**1**), CH=CH$_2$(**2**), CH$_2$–CH=CH$_2$(**3**), (CH$_2$)$_4$–CH=CH$_2$(**4**))
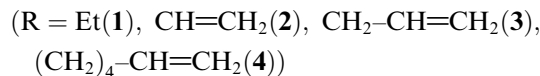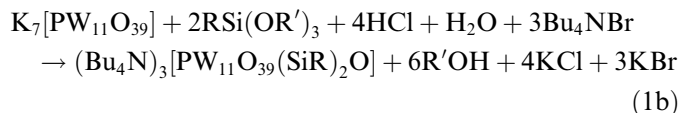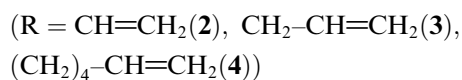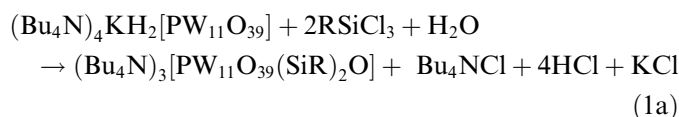
Tetrabutylammonium salts of the hybrid anions were isolated as air-stable white powders after several precipitations by ethanol/diethylether mixtures from acetonitrile solutions or by water from DMF solutions. These salts are very soluble in acetonitrile, acetone, DMF and DMSO, and poorly soluble in ether, pentane, water and ethanol. Attempts of recrystallization of the tetrabutylammonium salts in various solvents by several methods have been tried but always led to crystals non-suitable for X-ray analyses.

2.1.2. Hydrosilylation between **2** and $HSiEt_3$ or $HSiMe_2Ph$

$$[PW_{11}O_{39}(Si{-}CH{=}CH_2)_2O]^{3-} + 2R_2R'SiH$$
$$\rightarrow [PW_{11}O_{39}(Si{-}CH_2{-}CH_2SiR'R_2)_2O]^{3-}$$
$$(R = R' = Et(\mathbf{5}); \ R = Me, R' = Ph(\mathbf{6})) \quad (2)$$

It has been possible to extend the organic part of the hybrid compound $[PW_{11}O_{39}(SiCH{=}CH_2)_2O]^{3-}$ (**2**) by using the hydrosilylation reaction between **2** and two different silanes, $HSiEt_3$ and $HSiMe_2Ph$, which led respectively to the major (see below) products $[PW_{11}O_{39}(SiCH_2CH_2$-$SiEt_3)_2O]^{3-}$ (**5**) and $[PW_{11}O_{39}(SiCH_2CH_2SiMe_2Ph)_2O]^{3-}$ (**6**). The second-generation grafting could be achieved under reflux in a mixture THF/CH$_3$CN using the platinum Karstedt's catalyst (Fig. 2) [20]. At completion of the reaction, the products were isolated as air- and water-stable powders and analyzed by several spectroscopic methods.

2.2. Spectroscopic characterization of $[Bu_4N]_3[PW_{11}O_{39}(SiR)_2O]$

2.2.1. IR Spectroscopy

Infrared spectroscopy gives preliminary informations about the modification of the polyanionic structure. In the range 1200–300 cm^{-1}, all compounds **1**–**6** exhibit a spectrum similar to, but slightly different from that of the $[PW_{11}O_{39}]^{7-}$ precursor [18,19,21]. The two bands assigned to P–O vibrations of the central PO$_4$ tetrahedron are observed around 1065 and 1035–1040 cm^{-1} for **1**–**6**. They
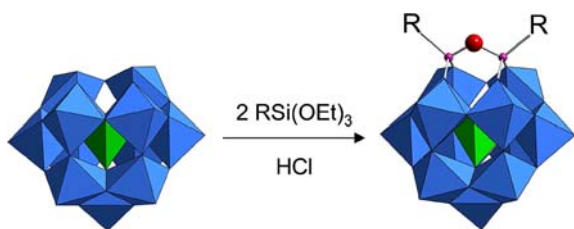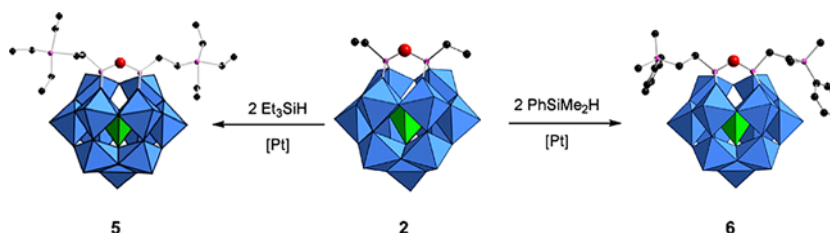

Fig. 2. Schematic procedure of hydrosilylation of **2** by Et$_3$SiH and PhMe$_2$SiH.

are shifted to low wavenumbers with respect to those of the tetrabutylammonium salt of $[PW_{11}O_{39}]^{7-}$ (1108 and 1052 cm^{-1}). The smaller Δv splitting (25–30 cm^{-1}) for **1**–**6**, instead of 56 cm^{-1} for $[PW_{11}O_{39}]^{7-}$, is in agreement with a partial saturation of the lacuna [21].

In the 1000–700 cm^{-1}, region of the W–O stretchings, most of the bands are shifted to high wavenumbers. These high frequency shifts are also characteristic of the saturation of the structure, as a consequence of the grafting of silyl groups.

The strong sharp band at 1112 cm^{-1} could be assigned to a Si–O–Si group [16,22]. In addition, the IR spectra exhibit weak features characteristic of the organic moiety.

These IR features indicate that the reaction leads to the grafting of RSi groups on the $[PW_{11}O_{39}]^{7-}$ anion, likely giving $[PW_{11}O_{39}(SiR)_2O]^{3-}$ as observed for $\{SiW_{11}\}$ derivatives [14]; nevertheless further spectroscopic investigations were performed to ensure this assumption.

In addition, the disappearance of the vibration assigned to the vinylic groups of **2** (at 1280 cm^{-1}) and the appearance of new weak bands at 1260 and 1241 cm^{-1} for **5**, and at 1249 and 3050 cm^{-1} for **6**, indicate that hydrosilylation of **2** occurred as expected. Moreover, the $\{PW_{11}O_{39}(Si)_2O\}$ backbone is not modified during hydrosilylation, since the chemical transformation occurred far enough to the inorganic $\{PW_{11}O_{39}\}$ skeleton.

2.2.2. Multinuclear NMR

2.2.2.1. ^{31}P NMR spectroscopy. For compounds **1**–**6**, one single narrow ^{31}P NMR signal at $\delta = -12.3 \pm 0.6$ ppm is observed, indicating that only one POM is present in the solution.

2.2.2.2. ^{1}H NMR spectroscopy. Between 6.3 and 4.7 ppm, the ^{1}H NMR spectra of compounds **2**–**4** exhibit the typical pattern characteristic of the ABX system of the CH=CH$_2$ vinylic group. The methylenic protons in the allyl- and
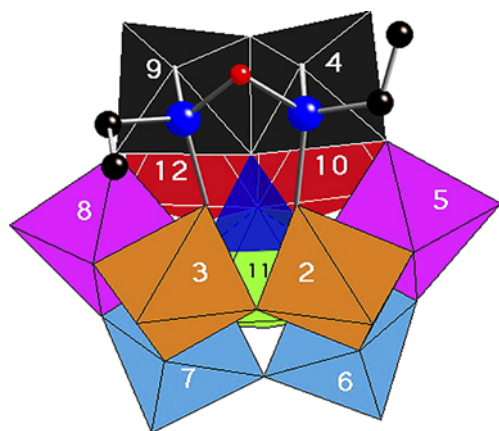

Fig. 3. Mixed representation of the postulated structure of $[PW_{11}O_{39}$-$(SiEt)_2O]^{3-}$ polyanion – The tungsten atoms have been labelled according to IUPAC conventions [23].

hexenyl-containing species appear in the classical range (0.7–4 ppm) but most of them are hidden by the strong signals of the tetrabutylammonium cations. In all the spectra, the integration of selected signals with respect to those of the tetrabutylammonium cations, agrees with two SiR fragments for three tetrabutylammonium cations. Moreover, the relative simplicity of the vinylic region argues for the equivalence of the two SiR groups. Therefore, the structure of the hybrid anion should consist of $\{PW_{11}O_{39}\}$ on which are symmetrically grafted two SiR groups connected through one Si–O–Si bridge. A schematic postulated structure of the $[PW_{11}O_{39}(SiCH_2CH_3)_2O]^{3-}$ anion is displayed in Fig. 3 with atom numbering according to IUPAC conventions [23].

^{1}H NMR spectroscopy also proves unambiguously the success of the hydrosilylation reaction. Actually, for **5** (resp. **6**), the signals of the vinylic groups are missing and new complex multiplets between 0.2 ppm and 0.7 ppm may be assigned to –SiCH$_2$CH$_2$Si– moieties as well as to –CH$_3$ of Et$_3$Si– (resp. Me$_2$Si) fragment. ^{29}Si NMR spectra (see below) show that minor species are also present, likely resulting from anti-Markovnikov addition; however the ^{1}H NMR cannot let us quantify the Markovnikov/anti-Markovnikov ratio, but is in favour of Markovnikov addition (see infra). The methylenic protons of the Et$_3$Si– fragment for **5** are observed as a quartet shouldering the triplet corresponding to the methyl group of tetrabutylammonium cations. Complete transformation of the vinylic group is also proved by integration of these signals with respect to those of the tetrabutylammonium cations, which agrees with two Et$_3$SiCH$_2$CH$_2$Si– (resp. PhMe$_2$SiCH$_2$CH$_2$Si–) fragments for three tetrabutylammonium counter-cations for **5** (resp. **6**).

2.2.2.3. ^{29}Si NMR spectroscopy. In agreement with the symmetrical postulated structure, the ^{29}Si NMR spectra of compounds **1**–**4** exhibit a single peak at $\delta = -50.3$, -64.9, -56.1 and -50.0 ppm for **1**, **2**, **3** and **4**, respectively, characteristic of SiO$_3$C environment (T groups) [24]. Moreover, this signal is flanked with satellites corresponding to a $^{2}J(^{29}Si-^{183}W)$ coupling constant of 12 Hz.

The variation of the ^{29}Si shift follows the trend observed for other RSi-containing species [24]. A stronger donor effect of the R moiety (hexenyl > ethyl > allyl > vinyl) [25] shifts the ^{29}Si signal towards higher frequencies.

The ^{29}Si NMR spectrum of **5** exhibits two main signals of same relative integrated intensity at $\delta = +8.9$ ppm and $\delta = -51.7$ ppm, attributable to **Si**C$_4$ (SiEt$_3$) and **Si**O$_3$C (Si(POM)), respectively. It is noteworthy that the ^{29}Si NMR signal corresponding to the vinylic substituted silicium atom (at $\delta = -64.9$ ppm) is strongly shifted towards less negative values, indicating a change of electronic environment (from Si–C(sp^2) to Si–C(sp^3)). Actually, the ^{29}Si NMR shift of Si(POM) in the case of **5** is also close to the SiEt signal observed for **1**. The relative integration of the signals (1/1) fits with the postulated formula of **5** and confirms the "saturation" of both vinylic groups.

Minor signals likely correspond to the anti-Markovnikov addition product as also observed for the hydrosilylation of simple compounds [20].

2.2.2.4. ^{183}W NMR spectroscopy. The ^{183}W NMR spectra of **1–4** are quite similar. They exhibit six doublets ($^{2}J(^{31}P–^{183}W)$ coupling between 1.1 and 1.6 Hz) at $\delta = -98 \pm 2$, -102 ± 2, -107 ± 2, -120 ± 1, -197 ± 2 and -249 ± 3 ppm with 2:2:1:2:2:2 intensities, respectively (Fig. 4) in agreement with C_s symmetry of a monosubstituted Keggin anion [26].

The ^{183}W NMR spectrum of **5** is consistent with the presence of two species, one major and one minor, both of C_s symmetry, with chemical shifts close to those of the former species **1–4**. This may be assigned to two structurally closely related derivatives resulting from the hydrosilylation reaction; the major product corresponding likely to Markovnikov addition while the minor one results from the sterically less favoured anti-Markovnikov addition [20].

2.2.2.5. Assignment of ^{183}W NMR spectrum of 1. As for other monosubstituted Keggin anions which present well resolved ^{183}W NMR 1D spectra, assignment of the different signals to the structurally non-equivalent tungsten atoms can be done with the help of homonuclear tungsten–tungsten coupling constants only. Actually, for all compounds **1–4**, narrow ^{183}W resonances ($\Delta v_{1/2} < 1$ Hz) allow the observation of the tungsten satellites and the access to direct measurements of the $^{2}J_{W–W}$ coupling constants, even in ^{31}P coupled spectra. For that purpose, abscissa expansions of the six-resonance signals of **1** are displayed in Figs. 5 and 6.

Let us recall that two types of $^{2}J(^{183}W–^{183}W)$ coupling constants can be observed depending on the geometry of the μ-oxo W–O–W bridge. Coupling constants are around 10 Hz for edge-sharing octahedra and around 20 Hz for
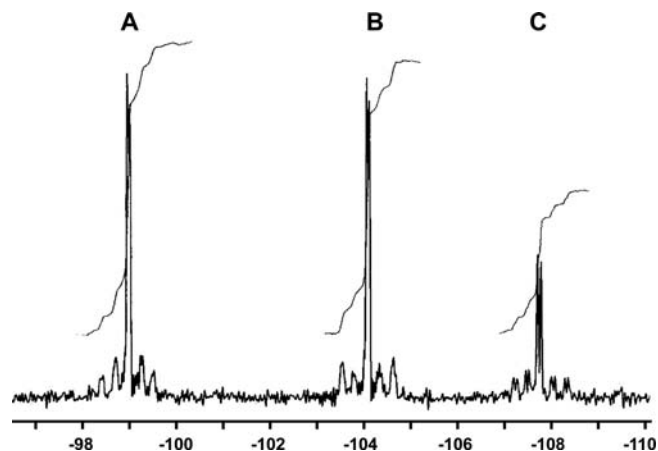

Fig. 5. Abcissa expansion of ^{183}W NMR signals **A**, **B** and **C**.
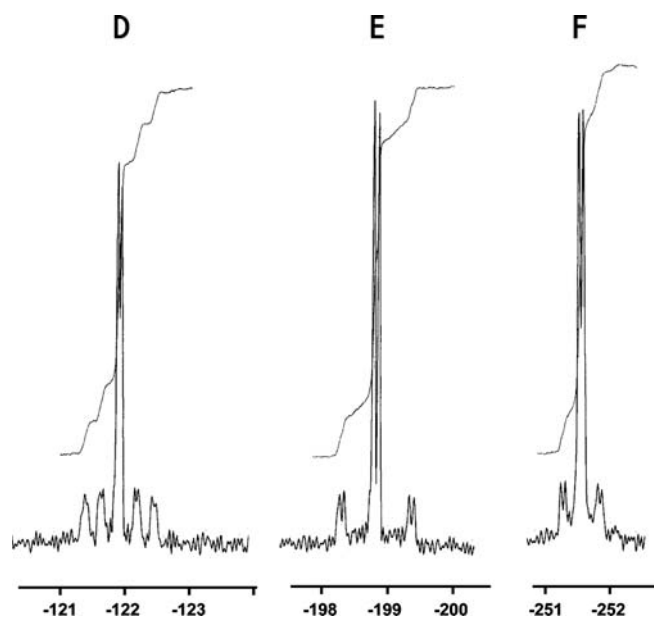

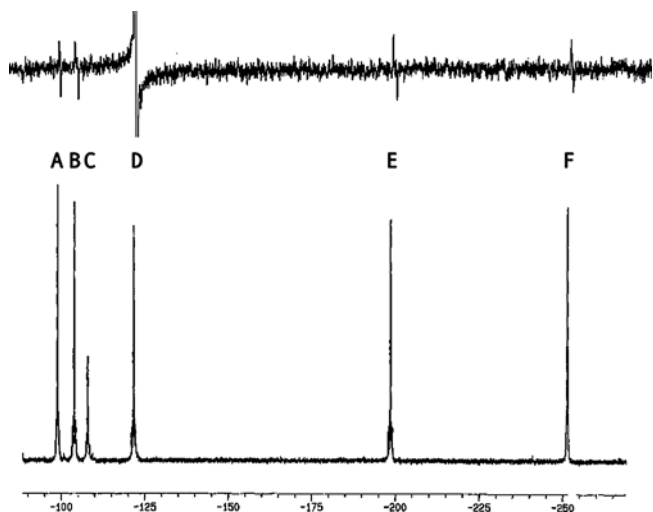Fig. 6. Abcissa expansion of ^{183}W NMR signals **D**, **E** and **F**.

corner-sharing octahedra [27]. On this basis, we can establish the theoretical connectivity matrix valid for any monosubstituted Keggin polytungstate (Table 1) [26].

Fig. 4. 12.5 MHz ^{183}W NMR of $[Bu_4N]_3[PW_{11}O_{39}(SiEt)_2O]$ (**1**): conventional 1D spectrum (down) and 1D COSY spectrum (up).

Table 1
Theoretical tungsten–tungsten connectivity matrix of $[PW_{11}O_{39}(SiR)_2O]^{3-}$

Nuclei	W2,3	W4,9	W5,8	W6,7	W10,12	W11
W2,3			w	w		
W4,9			S		S	
W5,8	w	S		w	S	
W6,7	w		w			S
W10,12		S	S			w
W11				S	w	

The strong ^{183}W-^{183}W coupling constants (around 20 Hz) are symbolized by **S** and the weak ones (around 10 Hz) by **w**.

The starting point for the assignment is signal **C** ($\delta = -108.0$ ppm) with relative intensity 1, assigned to *W11* lying in the symmetry plane (Figs. 4 and 5).

Both low-frequency signals **E** ($\delta = -198.7$ ppm) and **F** ($\delta = -251.5$ ppm) present only one pair of satellites corresponding in each case to a coupling with two tungsten neighbours, as shown by the relative integration of the satellites with respect to the central line (Fig. 6). The $^2J_{W-W}$ values are 22 and 11.7 Hz for **E** and **F**, respectively. According to the theoretical connectivity matrix, **E** and **F** are therefore assigned to *W4* (resp. *W9*) and *W2* (resp. *W3*). Theoretically, *W5* (resp. *W8*) should present four pair of satellites, two with small couplings and two with strong couplings. For *W6* (resp. *W7*) and *W10* (resp. *W12*), only three pairs of satellites are expected, i.e. with two weak and one strong coupling constants for *W6* (resp. *W7*), and two strong and one weak ones for *W10* (resp. *W12*). Experimentally, it occurs that all corner- (resp. edge-) coupling constants have similar values around 22 Hz (resp. 11 Hz). Therefore, the different satellites cannot be totally resolved. However, in that case, relative integration of the satellites with respect to the central line permits to discriminate between *W5* (resp. *W8*), *W6* (resp. *W7*) and *W10* (resp. *W12*). Even visual observation of the sub-spectra is sufficient to assign **A** ($\delta = -99.0$ ppm) to *W6* (resp. *W7*), **B** ($\delta = -104.0$ ppm) to *W10* (resp. *W12*) and **D** ($\delta = -121.8$ ppm) to *W5* (resp. *W8*) (Figs. 5 and 6). Assignment of **D** to *W5* (resp. *W8*) is confirmed by the 1D-COSY spectrum (Fig. 4 upper trace) which presents four antiphase doublets at **A**, **B**, **E** and **F** positions.

While the $^2J_{W-W}$ coupling constants take atypical values in lacunary POMs [26c,28], grafting of the SiR group on the {PW11} backbone restores the typical values observed in complete POM structures for edge- and corner-junctions (ca. 10 and 20 Hz, respectively).

Moreover, in the particular case of organosilyl derivatives of monovacant tungstates, it is noteworthy that the tungsten nuclei O-bonded to the silicon atoms are significantly shielded with respect to the remote W nuclei, which give ^{183}W signal in a very narrow range, not markedly shifted with respect to those of {PW11} signals.

2.3. Chromogenic studies of the hybrid species

Having in mind the use of these hybrid species to prepare chromogenic materials [14c,14d,14e], we have first performed a cyclic voltammetry.
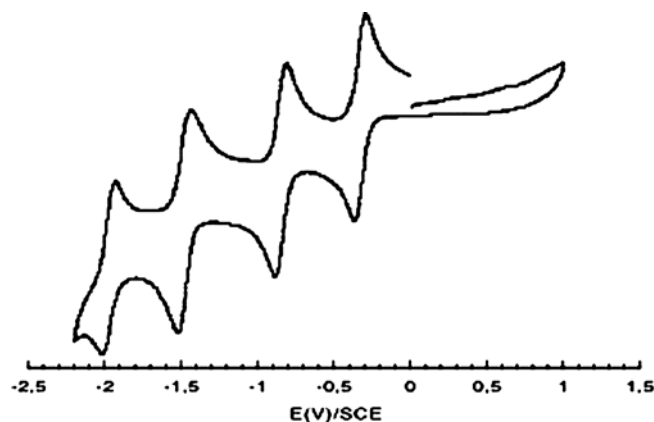

Fig. 7. Cyclic voltammogram of $\{Bu_4N\}_3[PW_{11}O_{39}(SiEt)_2O]$ (**1**) ([**1**] $= 1 \times 10^{-3}$ M in acetonitrile with 10^{-1} M Bu$_4$NBF$_4$ as supporting electrolyte).

2.3.1. Electrochemical measurements of the hybrid species

Since polyoxometalates are d^0 transition metals clusters, known to be usually easily reduced [7–11], we have investigated the electrochemical behaviour of several species by cyclic voltammetry in acetonitrile at a glassy carbon working electrode, using tetrabutylammonium tetrafluoroborate as supporting electrolyte and SCE as reference electrode.

The results are summarized in Table 2 and Fig. 7 displays a typical voltammogram for **1**.

Between 0 V and -2 V, four (resp. three) monoelectronic reduction waves are observed for **1** and **2** (resp. **5** and **6**). The first reduction corresponds to a quasi-reversible monoelectronic process between -0.32 V and -0.40 V vs. SCE. The shift to less negative values by comparison with the first reduction potential of $[PW_{11}O_{39}]^{7-}$ (-0.7 V) is consistent with the lowering of the charge of complete structures which become more easily reduced (compared with $[PW_{12}O_{40}]^{3-}$ -0.34 V). The first reduction potential is slightly dependent on the nature of the organic fragment grafted to the $[PW_{11}O_{39}]^{7-}$ subunit. As expected on the basis of their whole charge, the species reported herein are more easily reduced than the hybrid tungstosilicates reported by Judeinstein [14].

2.3.2. Chromogenic behaviour of the hybrid species in solution

Polyoxometalates are known to be interesting chromogenic units that can be used in several devices as well in solution as in the solid state [5–9,14]. In order to test the

Table 2
Redox potentials (vs SCE) of selected hybrid POMs[a]

Compound[a]	E(1)[b] ($\Delta E(1)$)[c]	E(2)[b] ($\Delta E(2)$)[c]	E(3)[b] ($\Delta E(3)$)[c]	E(4)[b] ($\Delta E(4)$)[c]
1	-0.32 V (*86* mV)	-0.85 V (*86* mV)	-1.50 V (*98* mV)	-1.99 V (*86* mV)
2	-0.33 V (*74* mV)	-0.85 V (*74* mV)	-1.48 V (*80* mV)	-1.97 V (*115* mV)
5	-0.40 V (*72* mV)	-0.92 V (*82* mV)	-1.56 V (*114* mV)	
6	-0.36 V (*130* mV)	-0.87 V (*130* mV)	-1.54 V (*140* mV)	

[a] [POM] $= 1 \times 10^{-3}$ M in acetonitrile with 10^{-1} M Bu$_4$NBF$_4$ as supporting electrolyte.

[b] $E(i) = 1/2(E(i)_{ox} + E(i)_{red})$.

[c] $\Delta E(i) = E(i)_{ox} - E(i)_{red}$.

chromogenic capacity of these hybrid species, we have studied their electrochemical and photochemical reduction.

2.3.2.1. Electrochromism. Reduction at a fixed potential of −0.6 V vs. ECS (for one electron reduction) of a $0.25.10^{-3}$ M solution of **2** in CH_3CN using 10^{-1} M Bu_4NBF_4 as supporting electrolyte leads to a blue solution. The UV–Vis spectrum of a reduced solution of **2** presents two bands at $\lambda = 480$ nm ($\varepsilon = 1120$ L mol^{-1} cm^{-1}) and $\lambda = 725$ nm ($\varepsilon = 2400$ L mol^{-1} cm^{-1}), respectively, corresponding to *d–d* transitions [9] (Fig. 8). The intervalence transfer should occur at lower energy in the near IR region.

At the early stage of the reduction process, the absorbance at 725 nm is proportional to the reduction time, which means that the rate of reduction remains nearly constant. This solution bleaches after electrochemical back-oxidation at 0 V or after air bubbling. This behaviour was observed for several cycles, demonstrating the stability of the polyanion in both oxidized and reduced forms.

2.3.2.2. Photochromism. The same compound has been tested for its photochromic properties. A DMF solution of **2** has been put into a quartz cell and irradiated using a 125 W Hg irradiation lamp. After a few minutes, a blue colouration appeared and the UV–Vis spectrum of the solution was similar to that of a electrochemically reduced solution. As for the electrolysis, the blue colouration increased with the exposure time and air exposure led to the bleaching of the solution. Because of the quenching effect of oxygen towards the reduced blue species leading to colourless species, it is well known that anaerobic conditions are in favour of the persistence of the blue colouration of the solution. Measurements done in non-degassed DMF showed a maximum of intensity then a decrease is observed subsequently. During the irradiation process, the oxygen dissolved in DMF is probably transformed into ozone, which immediately quenches any reduced species formed.

3. Conclusion

The organic part of the "simple" organosilylated POM $[PW_{11}O_{39}(Si–CH=CH_2)_2O]^{3-}$ may be extended by hydrosilylation. The new species still exhibit the chromogenic properties characteristic of the POM inorganic core. This may be especially interesting for the elaboration of POM-based chromogenic materials, containing covalently linked POMs.

4. Experimental

Silanes, $^nBu_4NBr$, Ph_4PBr, Karstedt catalyst and DMF were purchased from Aldrich and used as received.

$(Bu_4N)_4KH_2[PW_{11}O_{39}]$ was prepared following a procedure adapted from the literature from $K_7[PW_{11}O_{39}]\cdot14H_2O$ and tetrabutylammonium bromide [18,19]. Both precursors were checked by IR and compared to the literature data. Acetonitrile was distilled on CaH_2 under argon atmosphere prior use. THF was distilled on Na/benzophenone under dry inert atmosphere. All experiments were performed under dry nitrogen atmosphere. The IR spectra (4000–250 cm^{-1}) were recorded on a Bio-Rad FTS 165 IR FT spectrometer in KBr pellets. ^1H (300.13 MHz) and ^{31}P (121.5 MHz) NMR spectra were recorded at 300 K in 5 mm o.d. tube on a Bruker AC 300 spectrometer equipped with a QNP probehead. ^{29}Si (99.4 MHz) and ^{183}W (12.5 MHz) NMR spectra were recorded at 300 K in 10 mm o.d. tube on a Bruker Avance 500 spectrometer equipped with a VSP probehead (^{29}Si) and on a Bruker Avance 300 equipped with a special low-frequency VSP probehead (^{183}W). The chemical shifts are given according to the IUPAC convention, with respect to Me_4Si (^1H, ^{29}Si), H_3PO_4 (^{31}P) and 2 M Na_2WO_4 aqueous solution (^{183}W). Electrochemical measurements were performed using glassy carbon as working electrode, platinum as counter-electrode and SCE as the reference. Each studied product was dissolved in distilled acetonitrile at a concentration of 10^{-3} M using Bu_4NBF_4
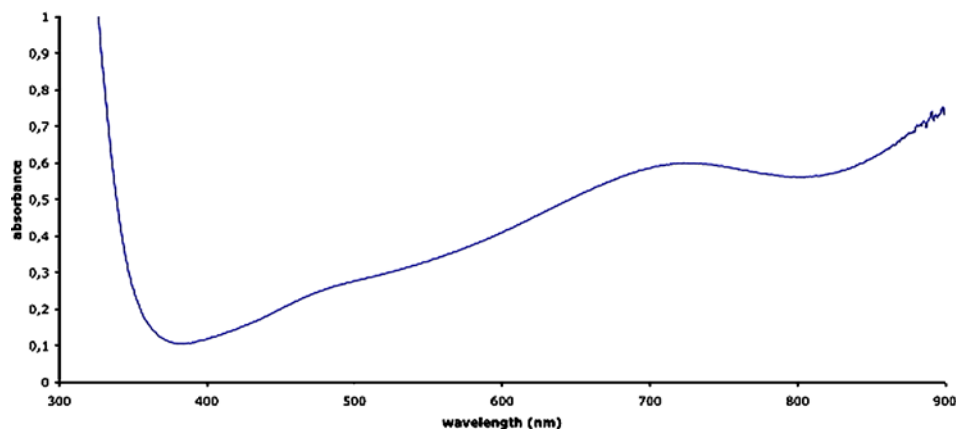

Fig. 8. Limit UV–vis spectrum of **2** after reduction at a fixed potential of −0.6 V vs. SCE ([**2**] = 0.25×10^{-3} M in acetonitrile with 10^{-1} M Bu_4NBF_4 as supporting electrolyte).

as electrolyte (10^{-1} M). The reduction was carried out at a fixed potential of -0.6 V vs. SCE using large area platinum electrodes. The coulometry experiments have been performed using an IG5-Tacussel integrator. Photochromic studies were performed by irradiation of a freshly degassed DMF solution of the hybrid POM by a 125 W Hg-lamp directly in the UV cell. UV–visible spectra were registered every 15 min.

4.1. Synthesis of $(Bu_4N)_3[PW_{11}O_{39}(SiEt)_2O]$ (**1**)

4.1.1. Method b

To a suspension of $K_7[PW_{11}O_{39}] \cdot 14H_2O$ (3.0 g, 0.93 mmol) in freshly distilled acetonitrile (30 mL) was added tetrabutylammonium bromide (1.5 g, 4.65 mmol). Then pure ethyltriethoxysilane (0.40 mL, 2.046 mmol) was added dropwise at 0 °C. A 2.4 M HCl solution (1,65 mL, 3.96 mmol) was added to the mixture. After one night of stirring at room temperature, volatiles were removed under vacuum. The solid obtained was redissolved in DMF, filtered and precipitated again several times by addition of water. The white precipitate of **1** was washed successively with ethanol and diethylether. Yield: 1.40 g (42%).

(**1**) ^{1}H NMR (CD$_3$CN) $\delta = 0.80$ (q, 4H, Si**CH$_2$**CH$_3$), 1.02 (t, 36H, (**CH$_3$**CH$_2$CH$_2$CH$_2$)$_4$N), 1.17 (t, 6H, SiCH$_2$**CH$_3$**), 1.50 (m, 24H, (CH$_3$**CH$_2$**CH$_2$CH$_2$)$_4$N), 1.85 (m, 24H, (CH$_3$CH$_2$**CH$_2$**CH$_2$)$_4$N), 3.45 (m, 24H, (CH$_3$CH$_2$CH$_2$-**CH$_2$**)$_4$N). ^{29}Si NMR (CH$_3$CN/CD$_3$CN) $\delta = -50.3$. ^{31}P NMR (CD$_3$CN) $\delta = -12.35$; ^{183}W NMR (CH$_3$CN/CD$_3$CN) $\delta = -251.6$ (2W, $^2J_{P–W} = 1.4$ Hz, $^2J_{W–W} = 11.7$ Hz (2W)), -198.8 (2W, $^2J_{P–W} = 1.6$ Hz, $^2J_{W–W} = 22$ Hz (2W)), -122.1 (2W, $^2J_{P–W} = 1.2$ Hz, $^2J_{W–W} = 11$ Hz (2W), $^2J_{W–W} = 22$ Hz (2W)), -108.3 (1W, $^2J_{P–W} = 1.5$ Hz, $^2J_{W–W} = 11$ Hz (2W), $^2J_{W–W} = 22$ Hz (2W)) -104.0 (2W, $^2J_{P–W} = 1.1$ Hz, $^2J_{W–W} = 11$ Hz (1W), $^2J_{W–W} = 22$ Hz (2W)), -99.2 (2W, $^2J_{P–W} = 1.1$ Hz, $^2J_{W–W} = 11$ Hz (2W), $^2J_{W–W} = 22$ Hz (1W)). IR (KBr pellets) $v = 1270$ (Si–C), 1112 (Si–O–Si), 1065 (P–O), 1036 (P–O), 982 (W=O), 964 (W=O), 868 (W–O–W), 823 (W–O–W), 392 and 346 (α-isomer signature). C$_{52}$H$_{118}$N$_3$O$_{40}$P$_1$Si$_2$W$_{11}$ (3535.01 g mol^{-1}); C Found 17.38 (calc. 17.67), H 3.33 (3.36) N 1.07 (1.19).

4.2. Synthesis of $(Bu_4N)_3\{PW_{11}O_{39}(SiCH=CH_2)_2O\}$ (**2**)

4.2.1. Method a

To a solution of $(Bu_4N)_4K[H_2PW_{11}O_{39}]$ (3.5 g, 0.96 mmol) in freshly distilled acetonitrile (35 mL) was added dropwise vinyltrichlorosilane (0.30 mL, 2.4 mmol) at room temperature. After one day of stirring, the yellow solution was filtered then precipitated by addition of an ethanol/ether mixture. The white powder obtained was redissolved in DMF and precipitated again several times by water, in order to remove the excess of hydrolyzed silane. The white precipitate of **2** was washed successively with ethanol and diethylether. Yield: 1.42 g (41%).

4.2.2. Method b

To a suspension of $K_7[PW_{11}O_{39}] \cdot 14H_2O$ (3.0 g, 0.93 mmol) in 30 mL of freshly distilled acetonitrile was added tetrabutylammonium bromide (1.5 g, 4.65 mmol). Then triethoxyvinylsilane (0.43 mL, 2.05 mmol) were added dropwise at 0°C. A 2.5 M HCl solution (1.6 mL, 4.00 mmol) was added to the mixture. After one night of stirring at room temperature, volatiles were removed under vacuum. The solid obtained was redissolved in DMF and precipitated again several times by addition of water. The white precipitate of **2** was washed with ethanol and ether. Yield: 2,85 g (87%).

(**2**) ^{1}H NMR (CD$_3$CN) $\delta = 1.02$ (t, 36H, (**CH$_3$**CH$_2$-CH$_2$CH$_2$)$_4$N), 1.50 (m, 24H, (CH$_3$**CH$_2$**CH$_2$CH$_2$)$_4$N), 1.80 (m, 24H, (CH$_3$CH$_2$**CH$_2$**CH$_2$)$_4$N), 3.45 (m, 24H, (CH$_3$CH$_2$-CH$_2$**CH$_2$**)$_4$N), 5.10–6.40 (3m, 6H, Si–**CH=CH$_2$**). ^{29}Si NMR (DMF/[D$_6$]acetone) $\delta = -64.9$. ^{31}P NMR (CD$_3$CN) $\delta = -12.2$. ^{183}W NMR (DMF/[D$_6$]acetone) $\delta = -246.2$ (2W), -195.2 (2W), -119.2 (2W), -105.9 (1W) -101.5 (2W), -97.2 (2W). IR (KBr pellets) $v = 1274$ (Si–C), 1112 (Si–O–Si), 1066 (P–O), 1039 (P–O), 983 (W=O), 964 (W=O), 871 (W–O–W), 824 (W–O–W), 392 and 346 (α-isomer signature). C$_{52}$H$_{114}$N$_3$O$_{40}$P$_1$Si$_2$W$_{11}$ (3531.06 g mol^{-1}); C 17.60 (calc. 17.69), H 3.61 (3.25) N 1.46 (1.19) %.

4.3. Synthesis of $(Bu_4N)_3[PW_{11}O_{39}(Si–CH_2–CH=CH_2)_2O]$ (**3**)

Compound **3** was obtained using the same procedure as for **2** (method a) replacing CH$_2$=CH–SiCl$_3$ by allyltrichlorosilane (0.35 mL, 0.45 mmol). Compound **3** was isolated as a white powder. Yield: 1.16 g (34%).

(**3**) ^{1}H NMR ([D$_6$]acetone) $\delta = 1.03$ (t, 36H, (**CH$_3$**CH$_2$-CH$_2$CH$_2$)$_4$N), 1.50 (m, 24H, (CH$_3$**CH$_2$**CH$_2$CH$_2$)$_4$N), 1.80 (m, 4H, Si**CH$_2$**CH=CH$_2$), 1.85 (m, 24H, (CH$_3$CH$_2$**CH$_2$**CH$_2$)$_4$N), 3.45 (m, 24H, (CH$_3$CH$_2$CH$_2$**CH$_2$**)$_4$N), 4.8–6.1 (m, 6H, SiCH$_2$**CH=CH$_2$**). ^{29}Si NMR (DMF/[D$_6$]acetone) $\delta = -56.1$. ^{31}P NMR (CD$_3$CN) $\delta = -12.3$. ^{183}W NMR (DMF/[D$_6$]acetone) $\delta = -247.4$ (2W), -195.2 (2W), -120.2 (2W), -106.6 (1W) -101.6 (2W), -97.0 (2W). IR (KBr pellets) $v = 1260$ (Si–C), 1112 (Si–O–Si), 1066 (P–O), 1037 (P–O), 983 (W=O), 964 (W=O), 871 (W–O–W), 824 (W–O–W), 392 and 348 (α-isomer signature).

4.4. Synthesis of $(Bu_4N)_3[PW_{11}O_{39}(Si((CH_2)_4-CH=CH_2)_2O]$ (**4**)

Compound **4** was obtained using the same procedure as for **2** (method a) replacing CH$_2$=CH–SiCl$_3$ by CH$_2$=CH–(CH$_2$)$_4$SiCl$_3$ (0.52 g, 0.45 mmol). Compound **4** was isolated as a white powder. Yield: 2.83 g (81%).

(**4**) ^{1}H NMR ([D$_6$]acetone) $\delta = 0.80$ (m, 4H, Si-**CH$_2$**), 1.03 (t, 36H, (**CH$_3$**CH$_2$CH$_2$CH$_2$)$_4$N), 1.50 (m, 24H, (CH$_3$**CH$_2$**CH$_2$CH$_2$)$_4$N), 1.60 (m, 4H, **CH$_2$**-CH=CH$_2$), 1.85 (m, 24H, (CH$_3$CH$_2$**CH$_2$**CH$_2$)$_4$N), 3.44 (m, 24H, (CH$_3$CH$_2$CH$_2$**CH$_2$**)$_4$N), 4.6–6.2 (3m, 6H, CH$_2$**CH=CH$_2$**). ^{29}Si NMR (DMF/[D$_6$]acetone) $\delta = -50.0$. ^{31}P NMR

(CD_3CN) $\delta = -12.4$. ^{183}W NMR (DMF/$[D_6]$acetone) $\delta = -251.9$ (2W), -199.8 (2W), -121.7 (2W), -108.2 (1W) -104.4 (2W), -99.2 (2W). IR (KBr pellets) $v = 1260$ (Si–C), 1112 (Si–O–Si), 1065 (P–O), 1039 (P–O), 983 (W=O), 964 (W=O), 871 (W–O–W), 822 (W–O–W), 391 and 344 (α-isomer signature).

4.5. Reaction of (2) with Et_3SiH

Compound **2** (0.5 g, 0.142 mmol) was filled up into a Schlenk tube on inert atmosphere with a 1/1 CH_3CN/THF mixture (10 mL). Et_3SiH (0.09 ml, 0.56 mmol) was added dropwise to the solution followed with two droplets of Karstedt's catalyst. After some minutes, the colour of the solution turned yellow then blue. The solution was left at 70°C during ten hours. The solution turned back yellow after cooling. The resulting solution was first dried using vacuum pump and the crude dissolved in pure acetonitrile. A yellowish solid was precipitated by addition of EtOH. The powder was purified in several steps dissolving it in the minimum amount of acetonitrile then precipitating a first fraction of the product by EtOH. The filtrate was kept and a second precipitation by Et_2O afforded the compound with a relative good yield as a beige powder.

(**5**) ^1H NMR (CD_3CN) $\delta = 0{,}20$ (m, 12H, $SiCH_2CH_3$), 0.50 (m, 8H, $SiCH_2CH_2Si$), 0.97 (t, 18H, $SiCH_2CH_3$), 1.03 (t, 36H, $(CH_3CH_2CH_2CH_2)_4N$), 1.43 (m, 24H, $(CH_3CH_2CH_2CH_2)_4N$), 1.70 (m, 24H, $(CH_3CH_2CH_2CH_2)_4N$), 3.25 (m, 24H, $(CH_3CH_2CH_2CH_2)_4N$). ^{29}Si NMR (CD_3CN) $\delta = -51.7$ (Si–POM), $+8.9$ (SiEt$_3$). ^{31}P NMR (CD_3CN) $\delta = -12.3$. ^{183}W NMR (CD_3CN/CH_3CN) $\delta = -250.2$ (2W), -197.3 (2W), -122.4 (2W), -108.8 (1W) -104.6 (2W), -99.2 (2W). IR (KBr pellets) $v = 1112$ (Si–O–Si), 1065 (P–O), 1036 (P–O), 981 (W=O), 963 (W=O), 869 (W–O–W), 824 (W–O–W), 392 and 346 (α-isomer signature).

4.6. Reaction of (2) with $PhMe_2SiH$

Compound **6** was obtained as a white powder using the same procedure as for **5** replacing Et_3SiH by $PhMe_2SiH$.

(**6**) ^1H NMR (CD_3CN) $\delta = 0.35$ (m, 12H, $(CH_3)_2Si$), 0.70 (m, 4H, CH_2Si), 1.02 (m, 36H, $(CH_3CH_2CH_2CH_2)_4N$), 1.20 (t, 4H, CH_2Si), 1.43 (m, 24H, $(CH_3CH_2CH_2CH_2)_4N$), 1.66 (m, 24H, $(CH_3CH_2CH_2CH_2)_4N$), 3.45 (m, 24H, $(CH_3CH_2CH_2CH_2)_4N$)), 7.37 (m, 4H, CH_{Ar}), 7.6 (m, 4H, CH_{Ar}), 7.93 (m, 2H, CH_{Ar}). ^{31}P NMR (CD_3CN) $\delta = -12.33$. IR (KBr pellets) $v = 1112$ (Si–O–Si), 1065 (P–O), 1035 (P–O), 982 (W=O), 963 (W=O), 870 (W–O–W), 824 (W–O–W), 392 and 346 (α-isomer signature).

References

[1] Part 8 D. Agustin, C. Coelho, A. Mazeaud, P. Herson, A. Proust, R. Thouvenot, Z. Anorg. Allg. Chem. 630 (2004) 2049.
[2] D.R. Rosseinsky, R.J. Mortimer, Adv. Mater. 13 (2001) 783.
[3] N.M. Rowley, R.J. Mortimer, Sci. Prog. 85 (2002) 243.
[4] C.M. Lampert, Mater. Today 7 (2004) 28.
[5] (a) M.T. Pope, Heteropoly and Isopoly Oxometalates, Springer-Verlag, New York, 1983;
(b) M.T. Pope, A. Müller (Eds.), Polyoxometalates from Platonic Solids to Anti-Retroviral Activity, Kluwer Academic Publishers, Dordrecht, the Netherlands, 1994;
(c) M.T. Pope, A. Müller (Eds.), Polyoxometalate Chemistry From Topology via Self-Assembly to Applications, Kluwer Academic Publishers, 2001;
(d) T. Yamase, M.T. Pope (Eds.), Polyoxometalate Chemistry for Nano-Composite Design, Nanostructure Science and Technology, Kluwer Academic/Plenum Publishers, Dordrecht, the Netherlands, 2002;
(e) C.L. Hill (Ed.), Special issue on polyoxometalates, Chem. Rev. 98 (1998).
[6] D.E. Katsoulis, Chem. Rev. 98 (1998) 359.
[7] T. Yamase, Chem. Rev. 98 (1998) 307.
[8] (a) M.T. Pope, in: D.B. Brown (Ed.), Mixed-Valence Compounds, Reidel Publishing Co, Dordrecht, the Netherlands, 1980, p. 365;
(b) B. Krebs, in: A. Müller, E. Diemann (Eds.), Transition Metal Chemistry, Verlag Chemie, Weinheim, Germany, 1981, p. 91;
(c) R.I. Buckley, R.J.H. Clark, Coord. Chem. Rev. 65 (1985) 167;
(d) C.J. Young, Coord. Chem. Rev. 96 (1989) 89.
[9] (a) J.-M. Fruchart, G. Hervé, J.-P. Launay, R. Massart, J. Inorg. Nucl. Chem. 38 (1976) 1627;
(b) C. Sanchez, J. Livage, J.-P. Launay, M. Fournier, Y. Jeannin, J. Am. Chem. Soc. 104 (1982) 3194;
(c) C. Sanchez, J. Livage, J.-P. Launay, M. Fournier, J. Am. Chem. Soc. 105 (1983) 6817;
(d) A. Chemseddine, C. Sanchez, J. Livage, J.-P. Launay, M. Fournier, Inorg. Chem. 23 (1984) 2609.
[10] (a) J.J. Altenau, M.T. Pope, R.A. Prados, H. So, Inorg. Chem. 14 (1975) 417;
(b) R.A. Prados, M.T. Pope, Inorg. Chem. 10 (1976) 2547;
(c) K. Piepgrass, J.N. Barrows, M.T. Pope, J. Chem. Soc., Chem. Commun. 1 (1989) 10;
(d) J.N. Barrows, G.B. Jameson, M.T. Pope, J. Am. Chem. Soc. 107 (1985) 1771.
[11] (a) M. Kozik, C.F. Hammer, L.C.W. Baker, J. Am. Chem. Soc. 108 (1986) 2748;
(b) M. Kozik, C.F. Hammer, L.C.W. Baker, J. Am. Chem. Soc. 108 (1986) 7627;
(c) J.F. Kirkby, L.C.W. Baker, J. Am. Chem. Soc. 117 (1995) 10010;
(d) N. Casañ-Pastor, L.C.W. Baker, J. Am. Chem. Soc. 114 (1992) 10384.
[12] D.C. Duncan, C.L. Hill, Inorg. Chem. 35 (1996) 5828.
[13] C. Sanchez, G.J. de Soler-Illia, F. Ribot, T. Lalot, C.R. Mayer, V. Cabuil, Chem. Mater. 13 (2001) 3061.
[14] (a) P. Judeinstein, C. Deprun, L. Nadjo, J. Chem. Soc. Dalton Trans. (1991) 1991;
(b) P. Judeinstein, H. Schmidt, J. Sol–Gel Sci. Technol. 3 (1994) 189;
(c) P. Judeinstein, P.W. Oliveira, H. Krug, H. Schmidt, Adv. Mater. Opt. Electron. 7 (1997) 123;
(d) P. Judeinstein, Chem. Mater. 4 (1992) 4;
(e) P. Judeinstein, J. Sol–Gel Sci. Technol. 2 (1994) 147.
[15] (a) C.R. Mayer, V. Cabuil, T. Lalot, R. Thouvenot, Angew. Chem., Int. Ed. 38 (1999) 3672;
(b) C.R. Mayer, V. Cabuil, T. Lalot, R. Thouvenot, Adv. Mater. 12 (2000) 417;
(c) C.R. Mayer, R. Thouvenot, T. Lalot, Macromolecules 33 (2000) 4433;

(d) C.R. Mayer, R. Thouvenot, T. Lalot, Chem. Mater. 12 (2000) 257;

(e) A.R. Moore, H. Kwen, E.A. Maatta, Chem. Commun. (2000) 1793;

(f) J. Kang, Z. Peng, X. Zhu, Y. Wei, D.R. Powell, Angew. Chem., Int. Ed. 44 (2005) 6902;

(g) B. Xu, M. Lu, J. Kang, D. Wang, J. Brown, Z. Peng, Chem. Mater. 17 (2005) 2841.

[16] W.H. Knoth, J. Am. Chem. Soc. 101 (1979) 2211.

[17] (a) D.A. Judd, R.F. Schinazi, C.L. Hill, Antiviral Chem. Chemother. 5 (1994) 410;

(b) S. Shigeta, S. Mori, J. Watanabe, M. Baba, A.M. Khenkin, C.L. Hill, R.F. Schinazi, Antiviral Chem. Chemother. 6 (1995) 114.

[18] G.S. Kim, K.S. Hagen, C.L. Hill, Inorg. Chem. 31 (1992) 5316.

[19] (a) R. Contant, Can. J. Chem. 65 (1987) 568;

(b) E.N. Yurchenko, L.G. Detusheva, L.P. Solov'yeva, G.N. Kustova, S.V. Tsybulya, T.P. Lazarenko, Zh. Strukt. Khim. 33 (1992) 48.

[20] D. Seyferth, D.Y. Son, A.L. Rheingold, R.L. Ostrander, Organometallics 13 (1994) 2682.

[21] C. Rocchiccioli-Deltcheff, R. Thouvenot, J. Chem. Res. (S) (1977) 46.

[22] N. Ammari, G. Hervé, R. Thouvenot, New J. Chem. 15 (1991) 607.

[23] (a) Y. Jeannin, Chem. Rev. 98 (1998) 51;

(b) Y. Jeannin, M. Fournier, Pure Appl. Chem. 95 (11) (1987) 1529.

[24] R.K. Harris, B.E. Mann (Eds.), NMR and The Periodic Table, Academic Press, London, 1978.

[25] N.L. Allinger, M.P. Cava, D.C. De Jongh, C.R. Johnson, N.A. Lebel, C.L. Stevens, Organic Chemistry, French., McGraw-Hill, 1975–1976, 159.

[26] (a) C. Brévard, R. Schimpf, G. Tourné, C.M. Tourné, J. Am. Chem. Soc. 105 (1983) 7059;

(b) P.J. Domaille, J. Am. Chem. Soc. 106 (1984) 7677;

(c) R. Contant, R. Thouvenot, Y. Dromzée, A. Proust, P. Gouzerh, J. Clust. Sci. 17 (2006) 317.

[27] J. Lefebvre, F. Chauveau, P. Doppelt, C. Brévard, J. Am. Chem. Soc. 103 (1981) 4589.

[28] (a) J. Canny, A. Tézé, R. Thouvenot, G. Hervé, Inorg. Chem. 25 (1986) 2114;

(b) E. Cadot, R. Thouvenot, A. Tézé, G. Hervé, Inorg. Chem. 31 (1992) 4128;

(c) C.R. Mayer, R. Thouvenot, J. Chem. Soc., Dalton Trans. (1998) 7.